

Boson Peak and High Frequency Modes in Amorphous Silica

Bertrand Guillot and Yves Guissani

Laboratoire de Physique Théorique des Liquides, (CNRS URA 765) Université Pierre et Marie Curie, Boîte 121, 4 Place Jussieu, 75252 Paris Cedex 05, France

(Received 10 June 1996)

Low and high frequency modes in fused silica at normal and very high density are investigated by molecular dynamics simulation. The calculated vibrational density of states, the Raman intensity, and the far infrared spectrum of normal silica glass present a low frequency mode ($\sim 50 \text{ cm}^{-1}$) whose shape and attenuation with temperature is closely related to the boson peak observed experimentally. This mode is attributed to concerted motions between SiO_4 tetrahedra. Finally, the present analysis supports the recent suggestion that silica glass becomes fragile at very high density. [S0031-9007(97)02759-2]

PACS numbers: 63.50.+x, 61.20.Ja, 61.20.Lc, 78.30.Jw

Three of the most challenging problems in glassy state theory are the elucidation of the molecular motions (individual and concerted) taking place in the picosecond and subpicosecond time scale, their connection with the mesoscopic scale, and their evolution along the route leading to the liquid state [1]. From the experimental point of view, optical spectroscopies (Raman [2] and infrared [3]) and inelastic neutron scattering [4] have been widely used in the last two decades to investigate low and high frequency excitations in a large variety of amorphous materials. Vitreous silica was particularly scrutinized due to its importance in geosciences and the glass industry. Nevertheless, although the aforementioned techniques are complementary to one another, their connection requires some theoretical assumptions. The usual way to proceed is to compare the optical spectra with the vibrational density of states (VDOS) deduced from inelastic neutron scattering data via a light-to-phonons coupling coefficient [5] which generally exhibits a nontrivial frequency dependence. In contrast, in a MD simulation (once a force field governing the system is determined) it is possible to evaluate any correlation function and power spectrum of interest simply from the computer generated trajectories of the molecules or atoms making up the simulated sample.

We have evaluated by MD the mean square displacements, the VDOS, the Raman, and the far infrared (FIR) spectrum of a model of fused silica originally proposed by Tsuneyuki *et al.* [6] (TTAM) to describe the various crystalline phases of silica. A minor modification of this model potential, recently introduced by us [7] (named TTAMm) to eliminate some shortcomings of the original potential, allows for the investigation of the entire range of the liquid phase (~ 2000 – $12,000$ K). In the present work the tetracoordinated silica (quartzlike) at normal density (2.2 g/cm^3) and moderately high density (2.5 and 2.7 g/cm^3) as well as the hexacoordinated silica (stishovitelike) at 4.0 g/cm^3 were simulated between room temperature and 4000 K to cover both the glassy and the liquid state ($T_g^{\text{sim}} \sim 1800$ – 2500 K [7]). The calculations were carried out with 256 SiO_2 units, the Coulombic interactions ($q_{\text{Si}} = +2.4e$, $q_{\text{O}} = -1.2e$)

being handled by an Ewald sum (for further details see Ref. [7]). Particular attention was paid at low temperatures to average different runs with independent initial conditions.

The temperature dependence of the mean square displacement is presented in Fig. 1. The results plotted on a log-log graph confirm those obtained by Shao and Angell [8] with a less accurate potential for silica. Thus for normal silica glass (2.2 g/cm^3) the evolution of $\langle r^2 \rangle$ with time is characterized by a strong overshoot near 0.2 – 0.3 ps followed by well shaped oscillations, a feature which persists even at T_g^{sim} (~ 1800 K) but disappears rapidly in the

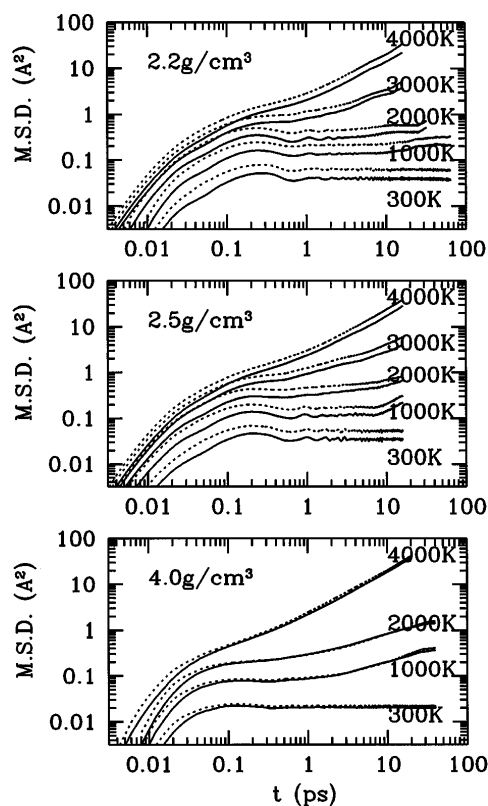


FIG. 1. Mean square displacements of silicon (bold curves) and oxygen (dotted curves) atoms in fused silica.

liquid state. In densified silica at 2.5 g/cm^3 the overshoot vanishes before T_g^{sim} , whereas at 2.7 g/cm^3 (not shown) the overshoot at room temperature and 1000 K is much less pronounced and the oscillations are strongly damped. In hexacoordinated silica at 4.0 g/cm^3 a different behavior is observed since neither an overshoot nor any oscillations show up in the glassy state. Moreover, when $\langle r^2 \rangle$ is plotted against the temperature (not shown) for a time matching the overshoot region (e.g., $t = 0.3 \text{ ps}$) a strict linearity is observed for all the polyamorphs up to T_g^{sim} (suggesting harmonic motions), whereas deviations from linearity occur at higher temperatures and are most pronounced when the density of the polyamorph is high. This means that on this time scale the dynamics becomes sensitive to anharmonicity and relaxation phenomena, a sensitivity which varies with the density of the polyamorph. To be complete, notice that although a change of the system size can affect the details of the relaxation dynamics in the picosecond time scale as shown recently [9], these finite size effects on the MSD are just sufficient to smooth somewhat the curves presented in Fig. 1, leaving unchanged the above conclusions.

In order to verify that the peculiar oscillations (and their damping) exhibited by $\langle r^2 \rangle$ are related to the famous boson peak (and its attenuation) observed by Raman spectroscopy [2] and inelastic neutron scattering [4], we have evaluated the neutron weighted VDOS, $g_N(\omega)$, a quantity directly connected to the mean square displacement of the atoms. The important point is that the quantity $g_N(\omega)/\omega^2$ can be identified (under specified conditions [10] and apart from unimportant factors) with the one-phonon scattering cross section as measured in neutron scattering experiments. It is striking to notice on Fig. 2 (see the log-log graph) that for normal silica glass the latter quantity evaluated by MD displays a pronounced peak in the boson peak region ($\sim 50 \text{ cm}^{-1}$), which decreases progressively with the temperature and is barely visible at liquid temperature (4000 K). In densified silica at 2.7 g/cm^3 the same trends are observed but the peak is slightly less pronounced than at normal density (not shown). By contrast, the hexacoordinated silica glass at 4.0 g/cm^3 shows a weak peak located at much higher frequency ($\sim 80 \text{ cm}^{-1}$) which disappears near T_g ($\sim 2500 \text{ K}$). The agreement between the simulation results and the neutron scattering data [4] for normal silica glass is striking. This means that the simulation is able to reproduce the observed boson peak and that its attenuation with the temperature is directly correlated to the damping of the oscillations in $\langle r^2 \rangle$, as suggested by Shao and Angell [8]. Furthermore, the fact that the simulation predicts a reduced boson peak for silica at stishovite density supports the conclusion that ultradensified silica glass is much more fragile than the normal glass (in general the amplitude of the boson peak is all the more weak when the glass is fragile [2]).

At higher frequency a detailed comparison with inelastic neutron scattering data [4] on normal silica glass shows (see Fig. 2) that the calculated VDOS agrees semiquan-

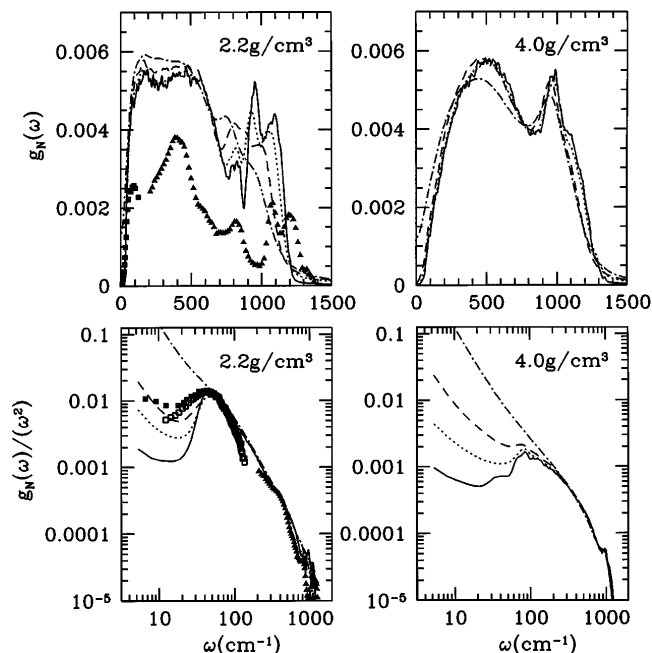


FIG. 2. Neutron weighted VDOS for fused silica at low and high density. The curves correspond to the total VDOS at $T = 300$ (bold), 1000 (dotted), 2000 (dashed), and 4000 K (dot-dashed), respectively. The filled squares represent the inelastic neutron scattering data of Buchenu *et al.* [4] and the empty squares that of Malinovsky *et al.* [4] for normal silica glass at room temperature, while the filled triangles are the corresponding high frequency data of Carpenter and Price [10]. The upper panels present linear plots of $g_N(\omega)$ and the lower panels are log-log plots of $g_N(\omega)/\omega^2$.

tatively with the experimental one. For example, the high frequency stretching band is located at too low a frequency ($\omega_{\text{sim}} - \omega_{\text{exp}} \sim -100 \text{ cm}^{-1}$) and the low frequency band ($100\text{--}600 \text{ cm}^{-1}$) is too flat, which indicates that the TTAM potential is not sufficiently accurate. On the other hand, the splitting of the 1000 cm^{-1} band and the deformation band near 800 cm^{-1} are remarkably well reproduced. A new feature appears in the evolution of the calculated VDOS with the temperature: It is the progressive redistribution of the intensity of the high frequency modes ($800\text{--}1100 \text{ cm}^{-1}$) in going from the glassy state to the liquid state. In ultradense silica at 4.0 g/cm^3 the situation is different in that the calculated VDOS changes very little in the glassy state (except the substantial redistribution of the vibration modes accompanying the change of coordination from fourfold to sixfold) and very rapidly above T_g (see Fig. 2), the very definition of a fragile behavior.

To elucidate the genesis of the boson peak and the high frequency modes found in the simulation of normal silica glass, we have evaluated by MD the VDOS associated first with an isolated $\text{SiO}_4^{2.4e}$ unit interacting via the TTAM potential and next when this unit is immersed in a frozen silica matrix (in the latter case, the VDOS was averaged over the 256 SiO_4 units available in our simulated sample). The VDOS of an isolated $\text{SiO}_4^{2.4e}$

unit shows four main bands (see the stick spectrum in Fig. 3), as expected for a T_d symmetry, located at 337, 504, 768, and 793 cm^{-1} , respectively, plus a number of much weaker combination bands. The effect of the vitreous field on these vibrational bands is considerable since in the frozen matrix not only are large frequency shifts observed (e.g., the symmetric stretching band which shifts from 793 to $\sim 950 \text{ cm}^{-1}$) but also broadening and interaction-induced splittings occur. However, the key point is that there is no boson peak in the low frequency region of the VDOS; the density of states has no contribution below 120 cm^{-1} when a fluctuating SiO_4 unit is incorporated in a frozen silica matrix (see Fig. 3). So the boson peak seen in the glass is the result of a collective excitation involving the concerted motions of several SiO_4 units.

Complementary information can be obtained from Raman and FIR spectroscopies. The infrared absorption coefficient is related to the Fourier transform $I(\omega)$ of the autocorrelation function of the total dipole moment by $\alpha(\omega) = \omega(1 - e^{-\hbar\omega/k_B T})I(\omega)$, where unimportant factors have been omitted. In the present case where Si and O ions possess a screened charge and are non-polarizable, $I(\omega)$ can be expressed rigorously in terms of the Fourier transform $g_J(\omega)$ of the autocorrelation function of the total charge current $\vec{J}(t) = \sum_i q_j \vec{v}_i(t)$,

namely $I(\omega) = g_J(\omega)/\omega^2$. Consequently, in the framework of the classical approximation (classical dynamics is required in a MD calculation) the following relation holds, $\alpha(\omega) = g_J(\omega)$. The calculated absorption spectrum for normal silica glass at room temperature is compared in Fig. 4 with the experimental data of Velde and Couty [11] beyond 400 cm^{-1} and with compilation data of Strom and Taylor [3] below 400 cm^{-1} . Here again the agreement is only semi-quantitative (a better agreement is obtained by Wilson *et al.* [12] in the 500 cm^{-1} region in using an interionic potential which includes polarization effects). As for the assignment of the spectral bands, note that in comparing $g_N(\omega)$ shown in Fig. 2 with the infrared absorption $g_J(\omega)$ of Fig. 4 some modes are canceled (e.g., near 800 cm^{-1}) while other are enhanced (e.g., near 600 cm^{-1}) by virtue of the selection rule imposed by the very definition of the collective variable \vec{J} . But the most interesting feature is the presence of a weak boson peak in the low frequency region of the FIR spectrum (see Fig. 4). This peak, although weak, was detected by Wong and Whalley [13] and other authors as reviewed by Strom and Taylor [3]. Moreover, the simulation also predicts that the peak disappears rapidly with increasing temperature (from 1000 K).

The Raman spectrum cannot be so easily evaluated because it requires supplementary information about

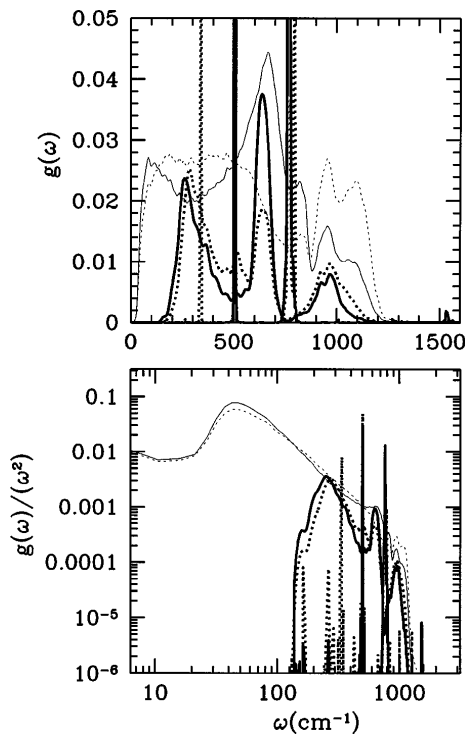


FIG. 3. The VDOS for an isolated $\text{SiO}_4^{-2.4e}$ tetrahedron (stick spectrum), a SiO_4 unit immersed in a frozen silica matrix (bold curves), and a silica glass at room temperature (thin curves). The continuous curves correspond to the motion of the silicons and the dotted curves to the oxygens. The upper panel is a linear plot of $g(\omega)$ and the lower panel a log-log plot of $g(\omega)/\omega^2$.

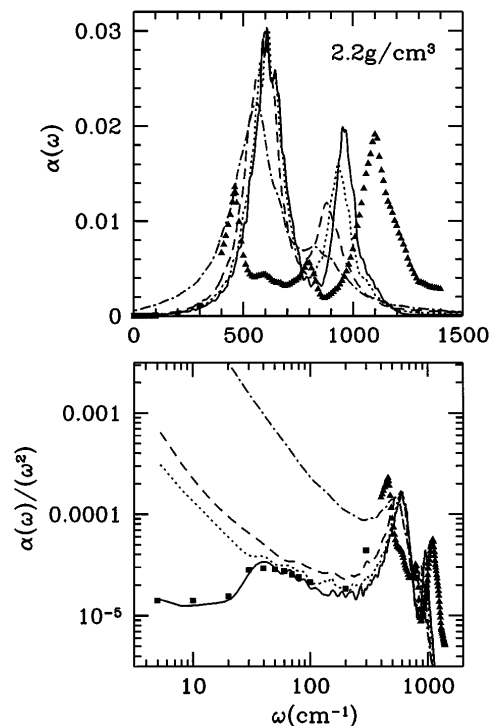


FIG. 4. The FIR spectrum of fused silica between room temperature and 4000 K (same symbols as in Fig. 2). The upper panel is a linear plot of the absorption coefficient $\alpha(\omega)$ and the lower panel a log-log plot of the intensity $\alpha(\omega)/\omega^2$. The filled triangles correspond to the experimental data of Ref. [11] and the filled squares to the data of Refs. [3,13].

interaction-induced polarizability in fused silica. Following Madden and Sullivan [14] it can be shown that several distinct mechanisms may contribute to the fluctuations in the total polarizability; distortion of the ions by Coulomb field gradient and field, overlap distortion between neighbors, and dipole-induced-dipole (DID) processes. In order to grasp the essence of the phenomena, the theory can be recast by using the SiO_4 units as the basic blocks of the glassy sample (the theoretical details will be given elsewhere [15]). In this framework the polarized Raman spectrum $I^{\text{VV}}(\omega)$ is essentially due to the frame distortion of the SiO_4 units while the depolarized spectrum $I^{\text{VH}}(\omega)$ is mainly caused by the DID mechanism between SiO_4 units. In the latter case the anisotropy of polarizability is given by $\pi^{\text{DID}} = \overline{\alpha_{\text{SiO}_4}} \sum_{i,j} \nabla \nabla (r_{i,j}^{-1})$ where i, j run over the silicon ions of the SiO_4 units, $r_{i,j}$ is the distance between two Si ions, and $\overline{\alpha_{\text{SiO}_4}}$ is the mean polarizability associated with SiO_4 units (in a first approximation $\overline{\alpha_{\text{SiO}_4}} = 4\alpha_O$ since the polarizability of the silicon ion is negligible with regard to that of the oxygen ion). In practice the evaluation by MD of the polarized Raman intensity gives a spectrum quite similar to the neutron weighted VDOS [see in Fig. 5 and compare with $g_N(\omega)$ in Fig. 2]. By contrast the depolarized Raman intensity

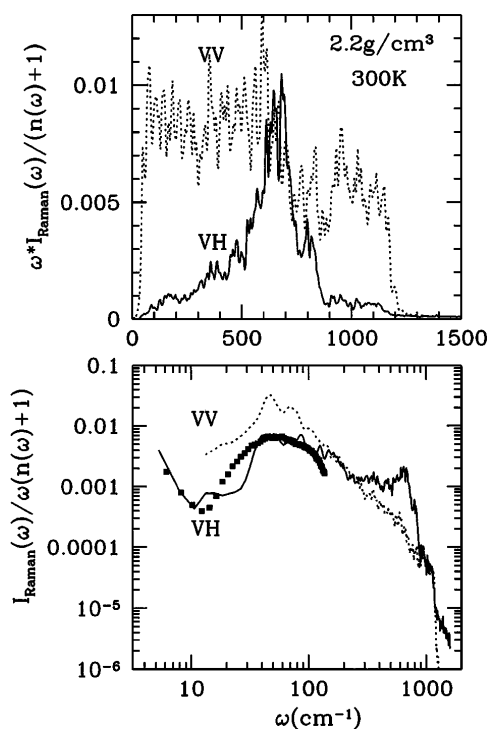


FIG. 5. The Raman spectrum of normal silica glass at room temperature: VH spectrum (bold curves), VV spectrum (dotted curves). The upper panel shows the reduced Raman intensity in a linear plot while the lower panel shows the temperature corrected Raman intensity [$n(\omega) + 1$ is the Bose factor] in a log-log representation. The experimental low frequency VH spectrum (squares) of Malinovsky *et al.* [4] is also shown for comparison. Notice the statistical noise of the calculated spectra due to the slow convergence of the simulated correlation functions.

is rather different since the intermediate frequency region ($500\text{--}900\text{ cm}^{-1}$) is magnified at the expense of the other spectral regions—a feature corroborated by the experimental data [16]. However, as far as the low frequency part of both spectra is concerned, the boson peak around 50 cm^{-1} is clearly present as expected, and its attenuation with temperature (not reported) is quite similar to that exhibited by the VDOS. But the important point is that the simulated VH spectrum which probes the medium-range order by the r dependence of π^{DID} is sensitive to the collective excitation related to Si-Si motions. Consequently, the boson peak is the result of concerted motions between SiO_4 units, this peculiar low frequency excitation disappearing as soon as one attempts to freeze the environment around a SiO_4 unit (see Fig. 2).

We thank the Institut du Développement et des Ressources en Informatique Scientifique (IDRIS, CNRS) for allocation of computer time on the CRAY C-98.

- [1] *Proceedings of the 2nd International Discussion Meeting on Relaxation in Complex Systems*, edited by K.L. Ngai, E. Riande, and G.B. Wright [J. Non-Cryst. Solids **172–174**, 420 (1994)].
- [2] A.P. Sokolov, E. Rossler, A. Kisliuk, and D. Quitmann, Phys. Rev. Lett. **71**, 2062 (1993).
- [3] U. Strom and P.C. Taylor, Phys. Rev. B **16**, 5512 (1977).
- [4] U. Buchenau, M. Prager, N. Nücker, A.J. Dianoux, N. Ahmad, and W.A. Phillips, Phys. Rev. B **34**, 5665 (1986); V.K. Malinovsky, V.N. Novikov, P.P. Parshin, A.P. Sokolov, and M.G. Zemlyanov, Europhys. Lett. **11**, 43 (1990).
- [5] F.L. Galeener, A.J. Leadbetter, and M.W. Stringfellow, Phys. Rev. B **27**, 1052 (1983).
- [6] S. Tsuneyuki, M. Tsukada, H. Aoki, and Y. Matsui, Phys. Rev. Lett. **61**, 869 (1988).
- [7] Y. Guissani and B. Guillot, J. Chem. Phys. **104**, 7633 (1996).
- [8] J. Shao and C.A. Angell, *Proceedings of the XVIIIth International Congress on Glass, 1995*; edited by Gong Fanglian (International Academic Publishers, Beijing, 1995), Vol. 1, p. 311; C.A. Angell, Comput. Mater. Sci. **4**, 285 (1995); Science **267**, 1924 (1995).
- [9] J. Horbach, W. Kob, K. Binder, and C.A. Angell, Phys. Rev. E **54**, 5897 (1996).
- [10] J.M. Carpenter and D.L. Price, Phys. Rev. Lett. **54**, 441 (1985).
- [11] B. Velde and R. Couty, J. Non-Cryst. Solids **94**, 238 (1987).
- [12] M. Wilson, P.A. Madden, M. Hemmati, and C.A. Angell, Phys. Rev. Lett. **77**, 4023 (1996).
- [13] P.T.T. Wong and E. Whalley, Discuss. Faraday Soc. **50**, 94 (1970).
- [14] P.A. Madden and K.F. O'Sullivan, J. Chem. Phys. **95**, 1980 (1991).
- [15] B. Guillot and Y. Guissani, Mol. Sim. (to be published).
- [16] P. McMillan, B. Piriou, and R. Couty, J. Chem. Phys. **81**, 4234 (1984).